Journal of Sound and Vibration (1998) **209**(1), 43–60

PERIODIC MOTIONS OF AN IMPACT OSCILLATOR

C. N. Bapat

Mechanical Engineering Department, The City College of the City University of New York, Convent Avenue at 138 West, New York, NY 10031, U.S.A.

(*Received* 28 *September* 1995, *and in final form* 17 *July* 1997)

Non-linear equations governing N impact periodic motions of a single-degree-of-freedom oscillator under a sinusoidal and bias force contacting rigid amplitude constraints on one or both sides have been developed with constant and velocity dependent coefficients of restitution. They also govern period doubling motions. Additionally, exact closed form expressions have been developed for one and two equispaced and non-equispaced impacts per cycle motions. Theoretical predictions agreed with previous results and with results obtained using a numerical simulation approach. Effects of amplitude and frequency of sinusoidal force, bias force, damping, and variable and constant coefficients of restitution on periodic motions are investigated.

1. INTRODUCTION

A single-degree-of-freedom impact oscillator model has been widely used for the last few decades as a first approximation to understanding the behavior of machines used in pile driving, compacting, crushing, rivetting, rock drilling, impact printing etc. [1–7]. For additional information the interested reader should refer to the papers listed in the bibliography. This model was also used to study the effects of snubbers and baffle plates which limit deflection of piping, and tubes in power, chemical and nuclear industries [8–11], as well as in marine structures [12–15]. Exact closed form solutions are available for a limited number of cases such as one equispaced impact/period motion of an oscillator contacting a single stop, and two alternating equispaced impacts with two stops during odd numbers of cycles and with a constant coefficient of restitution. Other complex periodic, period doubling and chaotic motions were extensively studied recently using theoretical and numerical simulation approaches [8–28]. Simulation approaches are computationally exhaustive in the study of periodic motions, especially when the system is lightly damped and stops are elastic. The goal of this study is to develop an exact approach to study complex periodic motions.

Non-linear equations governing N impacts/period of motion of a single-degree-of-freedom impact oscillator under a sinusoidal and bias force and contacting rigid amplitude constraints on one or on both sides were developed with velocity dependent coefficients of restitution. The impact duration was considered negligible. Also, N simplified equations for the widely used constant coefficient of restitution case were developed. In addition a novel closed form solution for two non-equispaced impacts/period of motion of these systems which includes the first period doubling motion of oscillator contacting a single stop and two alternating impacts per period of motion with two stops is presented. Theoretical predictions were checked with results obtained using a numerical simulation approach and with previous results, and they agreed. Effects of amplitude and frequency of sinusoidal force, bias force, damping, and variable and constant coefficients of restitution on periodic motions were investigated.

0022–460X/98/010043 + 18 $25.00/0/sv971230

2. THEORY

The model of an impact oscillator shown in Figure 1 consists of a primary mass M excited by an external sinusoidal force $F \sin \Omega t$ and a bias force F_0, a linear spring with stiffness K and a viscous dashpot having damping constant C. Rigid stops are located at distances S_1 on the right and S_2 on the left and were measured from an unstretched spring position. The differential equation of motion of mass M between impacts is

$$\ddot{X} + 2\xi\omega\dot{X} + \omega^2 X = (F/M) \sin \Omega t + F_0/M, \tag{1}$$

where X is the absolute displacement of M and the superscript dot represents the time derivative. Undefined variables in this and subsequent expressions are given in Appendix A. It can be shown that the displacement and velocity of M between the ith and the $(i+1)$th impacts can be expressed as [29]

$$X(t) = C_{1t}\, a_i + C_{2t}\, b_i + A \sin(\Omega t + \tau) + F_0/K, \tag{2}$$

and

$$\dot{X}(t) = C_{3t}\, a_i + C_{4t}\, b_i + A\Omega \cos(\Omega t + \tau), \quad t_{ia} \leqslant t \leqslant t_{(i+1)b}, \tag{3}$$

respectively. The subscript i, ia and ib represent quantities at, just after and just before the ith impact, respectively. It was assumed that a periodic motion with N impacts per period T_0 has been established with the known sequence of impacts on the right and left stop. The assumed impact sequence at unknown impact instants t_i respresents the impact pattern, i.e., the displacement of mass M at these impacts. This pattern is given by $X(t_i) = X_i = d_i$, where d_i takes values S_1 and $-S_2$ for impact on the right and left stop, respectively. As an example for $N = 4$, the sequence $d_i = 1, -1, 1, -1$ and $T_0 = 4\pi/\Omega$ indicates that the motion repeats after four impacts in two cycles and mass M hits stops alternatively. The $N-1$ contact instants $\alpha_i = \Omega t_i$, $i = i, 2, \ldots, N-1$, with $\alpha_1 = 0$ and τ, the phase angle of the assumed first impact, were considered unknowns. N coupled non-linear equations in the above mentioned N unknowns are developed by eliminating all other unknowns using the relation between velocity just after and before impact and is presented in what follows.

Displacement and velocity of M just before the $(i+1)$th impact X_{i+1} and $\dot{X}_{(i+1)b}$ can be obtained by substituting t_{i+1} for t in equations (2) and (3), respectively, as

$$X_{i+1} = d_{i+1} = C_{1i}\, a_i + C_{2i}\, b_i + A \sin(\alpha_{i+1} + \tau) + F_0/K, \tag{4}$$

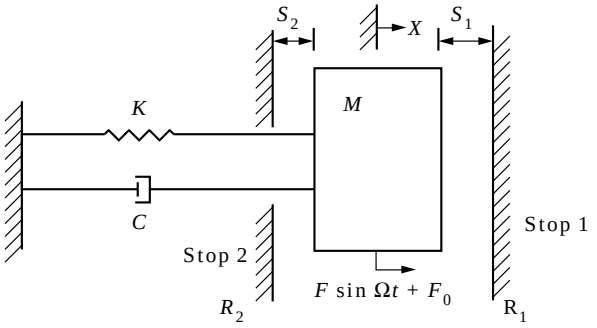

Figure 1. A single-degree-of-freedom impact oscillator with rigid amplitude constraints under external sinusoidal and bias force.

and

$$\dot{X}_{(i+1)b} = C_{3i}\, a_i + C_{4i}\, b_i + A\Omega \cos(\alpha_{i+1} + \tau), \quad i = 1, 2, \ldots, N. \tag{5}$$

The velocity of M just after the $(i+1)$th impact, $\dot{X}_{(i+1)a}$, can be obtained from equation (4) by substituting $i+1$ for i and using the value of a_{i+1} given in Appendix A. Further simplification leads to

$$\begin{aligned}\dot{X}_{(i+1)a} = {} & A \sin(\alpha_{i+1} + \tau)\,(\xi\omega + \eta\omega C_{2(i+1)}/C_{1(i+1)}) + A \sin(\alpha_{i+2} + \tau)\,(-\eta\omega/C_{1(i+1)}) \\ & + A\Omega \cos(\alpha_{i+1} + \tau) + (d_{i+1} - F_0/K)\,(-\xi\omega - \eta\omega C_{2(i+1)}/C_{1(i+1)}) \\ & + (d_{i+2} - F_0/K)/(\eta\omega/C_{1(i+1)}).\end{aligned} \tag{6}$$

$\dot{X}_{(i+1)b}$ can be expressed by rearranging equation (5) and using expressions of a_i and b_i from Appendix A as

$$\begin{aligned}\dot{X}_{(i+1)b} = {} & A \sin(\alpha_i + \tau)\,(C_{3i}\, C_{2i}/C_{1i}) + A \sin(\alpha_{i+1} + \tau)\,(-C_{3i}/C_{1i}) \\ & + A\Omega \cos(\alpha_i + \tau) + (d_i - F_0/K)\,(C_{3i}\, C_{2i}/C_{1i}) + (d_{i+1} - F_0/K)\,(C_{3i}/C_{1i}).\end{aligned} \tag{7}$$

The coefficient of restitution relates the velocity of M just before impact to its velocity after impact. The impact process can be complex and depends on many factors such as the approach velocity, contact geometry etc. [30, 31]. The prediction of the coefficient of restitution is difficult. However, previous research indicates that approximate models based on a linear or exponential variation of the coefficient of restitution with the approach velocity, expressed as

$$R_{i+1} = R_0\,(1 - k_1\, \dot{X}_{(i+1)b}) \quad \text{and} \quad R_{i+1} = R_0\,[(1 - k_2 \exp(-k_3\, \dot{X}_{(i+1)b})], \tag{8a, b}$$

are reasonable. Constants k_1, k_2 and k_3 can be obtained from the graph of the approach velocity versus the coefficient of restitution. A relation between $\dot{X}_{(i+1)a}$ and $\dot{X}_{(i+1)b}$ can be obtained using the Newtonian definition of the coefficient of restitution as

$$\dot{X}_{(i+1)a} = -R_{i+1}\, \dot{X}_{(i+1)b}, \quad i = 1, 2, \ldots, N. \tag{9}$$

For the velocity dependent coefficient of restitution case the N general equations governing the N impacts/period of motion in $N-1$ α_i's and τ can be obtained after substituting the expressions of $\dot{X}_{(i+1)b}$, $\dot{X}_{(i+1)a}$ and R_{i+1} from equations (6), (7) and (8), respectively, into equation (9). These general equations, however, can be simplified for a case of non-identical constant coefficients of restitution as follows. In this case R_i equals coefficients of restitution R_1 or R_2 for stop 1 and 2, respectively, and the pattern of R_i must be obtained from the assumed impact pattern d_i. After an algebraic manipulation, the resulting N equations can be expressed as

$$\begin{aligned}& A \sin(\alpha_i + \tau)\,[R_{i+1}\,(C_{4i} - C_{3i}\, C_{2i}/C_{1i})] + A \sin(\alpha_{i+2} + \tau)\,[\eta\omega/C_{1(i+1)}] \\ & + A \sin(\alpha_{i+1} + \tau)\,[R_{i+1}\, C_{3i}/C_{1i} - \xi\omega - \eta\omega C_{2(i+1)}/C_{1(i+1)}] \\ & + A \cos(\alpha_{i+1} + \tau)\,[-\Omega(1 + R_{i+1})] - (d_i - F_0/K)\,[R_{i+1}\,(C_{4i} - C_{3i}\, C_{2i}/C_{1i})] \\ & - (d_{i+1} - F_0/K)\,[R_{i+1}\, C_{3i}/C_{1i} - \xi\omega - \eta\omega C_{2(i+1)}/C_{1(i+1)}] \\ & - (d_{i+2} - F_0/K)\,[\eta\omega/C_{1(i+1)}] = 0, \quad i = 1, 2, \ldots, N.\end{aligned} \tag{10}$$

The case of identical coefficients of restitution can be studied using all $R_i = R$. The above two equations (9) and (10) can be used for all values of N. Cases covered by these equations include one equispaced, two non-equispaced, second and further period doubling motions of an oscillator contacting a single stop, the first period doubling motion of the oscillator

TABLE 1

Comparison of theoretical and simulation results. System parameters: $K = M = 1$ and $\xi = 0{\cdot}05$

Number of stops	Input variables	Type of motion		Exact solution: Equation (13)		Exact solution: Equations (9) and (10)		Digital simulation	
One	$F = 20, S_1 = 1{\cdot}0$	$N = 2$	$\alpha_i + \tau$	1·3833,	5·9644	1·3833,	5·9644	1·3833,	5·9644
	$\Omega = 1{\cdot}0, R_i = 0{\cdot}5$	$\Omega T_0 = 2\pi$	X_{ia}	−6·7548,	−19·3803	−6·7548,	−19·3803	−6·7548,	−19·3803
	$F = 1, S_1 = 0{\cdot}0$	$N = 4$	$\alpha_i + \tau$	—		2·0187,	7·1404	2·0187,	7·1404
	$\Omega = 2{\cdot}73, R_i = 0{\cdot}8$	$\Omega T_0 = 8\pi$				14·5534,	19·540	14·5534,	19·54
			X_{ia}			−0·3542,	−0·3616	−0·3541,	−0·3616
						−0·3119,	−0·3917	−0·3119,	−0·3917
Two	$F = 2, S_1 = 1{\cdot}0$	$N = 2$	$\alpha_i + \tau$	−0·01539,	3·2062	−0·01539,	3·2062	−0·0154,	3·2062
	$S_2 = 1{\cdot}05, \Omega = 1{\cdot}0$	$\Omega T_0 = 2\pi$	X_{ia}	−0·9592,	1·077	−0·9592,	1·077	−0·9592,	1·077
	$R_i = 0{\cdot}5$								
	$F = 4, S_1 = S_2 = 1{\cdot}0$	$N = 4$	$\alpha_i + \tau$	—		1·8351,	2·9441	1·8352,	2·9440
	$\Omega = 1{\cdot}1, R_i = 0{\cdot}5$	$\Omega T_0 = 2\pi$				4·9253,	5·9839	4·9253,	5·9839
			X_{ia}			1·5750,	0·6407	1·5750,	0·6407
						−1·5162,	−0·6480	−1·5162,	−0·6480

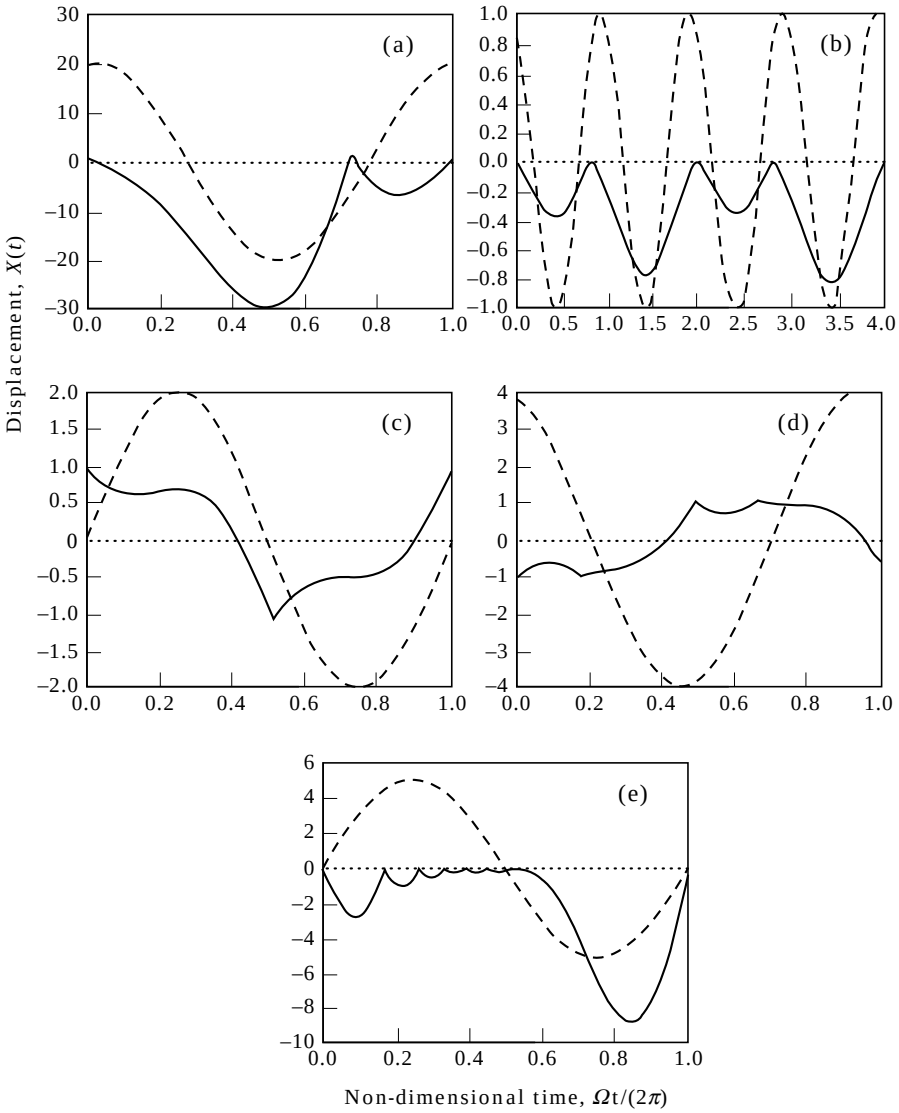

Figure 2. Displacement traces of periodic motions presented in Table 1: (a) unequispaced (2, 1); (b) period doubling (4, 4); (c) alternating (2, 1); (d) alternating (4, 1) with two consecutive impacts on the same side; (e) (6, 1) with velocity dependent coefficient of restitution. ——, displacement; and ----, external force.

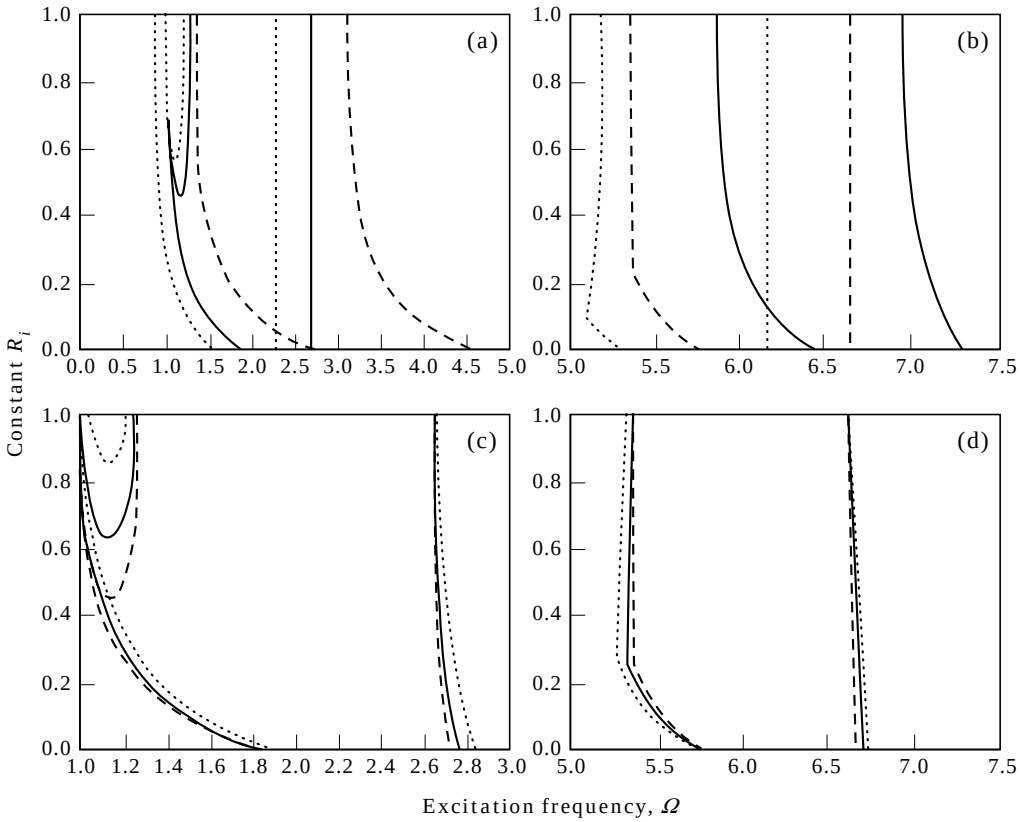

Figure 3. Effect of bias force on the stability regions of: (a) (1, 1) for $F_0 = 0{\cdot}0$, ——, $0{\cdot}2$, -----; $-0{\cdot}2$, – - –; (b) (1, 3) for $F_0 = 0{\cdot}0$, ----; $0{\cdot}025$, ——; $-0{\cdot}025$, – - –, at $\xi = 0{\cdot}0$ and $S_1 = 0$; and that of damping on: (c) (1, 1) and (d) (1, 3) with $\xi = 0{\cdot}0$, ----; $0{\cdot}05$, ——; $0{\cdot}1$, – - –, at $F_0 = 0{\cdot}0$ and $S_1 = 0{\cdot}0$.

contacting two stops and other multi-impact motions. Equations (9) and (10) were solved iteratively for all N using a Harwell library subroutine NS01A [32]. Iterations to obtain the unknowns continued until the sum of squares of the differences between the right and left sides of these equations was less than 10^{-14}.

However, for motions with two non-equispaced impacts per period, exact closed form expressions are developed in what follows. These include the following two motions of an impact oscillator contacting a single stop: (1) two impacts per period ($T_0 = 2\pi k$, $k = 1, 2, \ldots, d_i = S_1, \quad R_i = R_1$ and $\Omega t_i \neq \pi k$); and (2) first period doubling ($T_0 = 4\pi k$, $k = 1, 2, \ldots, d_i = S_1$, $R_i = R_1$ and $\Omega t_i \neq 2\pi k$); and an oscillator alternatively contacting two stops once on each side ($T_0 = 2\pi k$, $k = 1, 2, \ldots, d_1 = S_1$, $d_2 = -S_2$ and $\Omega t_i \neq \pi k$). In these cases equation (10) simplifies to

$$q_1 A \cos(\tau) + q_2 A \sin(\tau) = q_3, \quad q_4 A \cos(\tau) + q_5 A \sin(\tau) = q_6. \qquad (11a, b)$$

Equation (11) contains two unknowns τ and α_2 and can be further simplified by eliminating τ as

$$(q_3 q_5 - q_2 q_6)^2 + (q_3 q_4 - q_6 q_1)^2 = A^2(q_1 q_5 - q_2 q_4)^2$$

or

$$A = [\{(q_3 q_5 - q_2 q_6)^2 + (q_3 q_4 - q_6 q_1)^2\}/(q_1 q_5 - q_2 q_4)^2]^{1/2} \tag{12a, b}$$

This is a single equation in a single unknown α_2. To study two non-equispaced impact/period of motion when the applied force F is given, iteratively solving equation (12a) is more efficient than solving equation (10). The closed form of equation (12b) is most efficient to develop stability charts as α_2 can be assumed and A calculated without iterative computations.

Widely studied symmetric motion of an impact oscillator contacting each stop once with two alternating equispaced impacts/k cycles ($T_0 = 2\pi k$, $\alpha_{i+1} - \alpha_i = \pi k$) can occur only when $k = 1, 3, 5, \ldots$, $S_1 - F_0/K = S_2 + F_0/K = (S_1 + S_2)/2$ and all $R_i = R$, i.e., k is odd and the effective gaps and coefficients of restitution are equal. In this case equations (11a) and (11b) are identical and lead to a single equation in τ as

$$\sin\tau + \{\Omega(1+R)C_{11}/[\eta\omega - RC_{31}) \quad (C_{21}+1) + C_{11}(\xi\omega + RC_{41})]\}\cos\tau = (S_1 - F_0/K)A. \tag{13}$$

This equation agrees with the previous research where $S_1 = S_2$ and $F_0 = C = 0$.

Another important case is that of one equispaced impact per k cycles of motion of an impact oscillator contacting a single stop, i.e., $\alpha_{i+1} - \alpha_i = 2\pi k$, $k = 1, 2, 3, \ldots$, and $R_i = R =$ constant. In this case $N = 1$ and equation (10) simplifies significantly and can be expressed as

$$\sin\tau + \{\Omega(1+R)C_{11}/[(\eta\omega + RC_{31})(C_{21} - 1) + C_{11}(\xi\omega - RC_{41})]\}\cos\tau = (S_1 - F_0/K)/A, \tag{14}$$

and agrees with the previous research where $C = F_0 = 0$.

The stability of periodic motion was investigated by finding the eigenvalues of matrix P, where $P = P_i P_{i+1} \ldots P_{i+N}$. The P_i relates the perturbations $\Delta\alpha_{i+1}$ and $\Delta\dot{X}_{(i+1)a}$, respectively, in α_{i+1} and $\dot{X}_{(i+1)a}$ at the $(i+1)$th impact to the corresponding perturbations at the ith impact as

$$\begin{bmatrix} \Delta\alpha_{i+1} \\ \Delta\dot{X}_{(i+1)a} \end{bmatrix} = \begin{bmatrix} P_i(1,1) & P_i(1,2) \\ P_i(2,1) & P_i(2,2) \end{bmatrix} \begin{bmatrix} \Delta\alpha_i \\ \Delta\dot{X}_{ia} \end{bmatrix}. \tag{15}$$

Closed form expressions of P_i are given in Appendix A for the velocity dependent and constant coefficients of restitution cases. Periodic motion is asymptotically stable if and only if all eigenvalues of P lie within the unit circle in the complex plane. In addition to satisfying stability conditions, motion must satisfy other physical requirements such as velocity after impact being away from the wall, i.e.,

$$\dot{X}_{ia} < 0 \text{ for } X(t_i) = S_1 \qquad \text{and} \qquad \dot{X}_{ia} > 0 \text{ for } X(t_i) = -S_2. \tag{16}$$

Equation (16) will eliminate wall penetrating motions. Additionally the displacement of M between impacts must be within stops, i.e.,

$$-S_2 < X(t) < S_1. \tag{17}$$

Violation of the last condition indicates that more than N impacts occur within the considered period and this fact can be used to obtain the end point of N impacts/period of motion.

A completely numerical approach was also used to validate theoretical predictions. The complete time history of motion was obtained using zero initial values of X_1, $\dot{X}_{1a}$, t_1, Z_1 and using $\dot{Z}_{1a} = \pm 4$ units/s unless stated otherwise. Next, the contact instant t_2 was obtained by iteratively solving $|X(t_2) - S_1 \text{ or } +S_2| \leqslant 10^{-8}$. $\dot{X}_{2b}$ was obtained using equation (3) and $\dot{X}_{2a}$ using equations (8) and (9). New initial conditions were obtained at t_2 and the process was continued for a sufficiently long time. All computations were

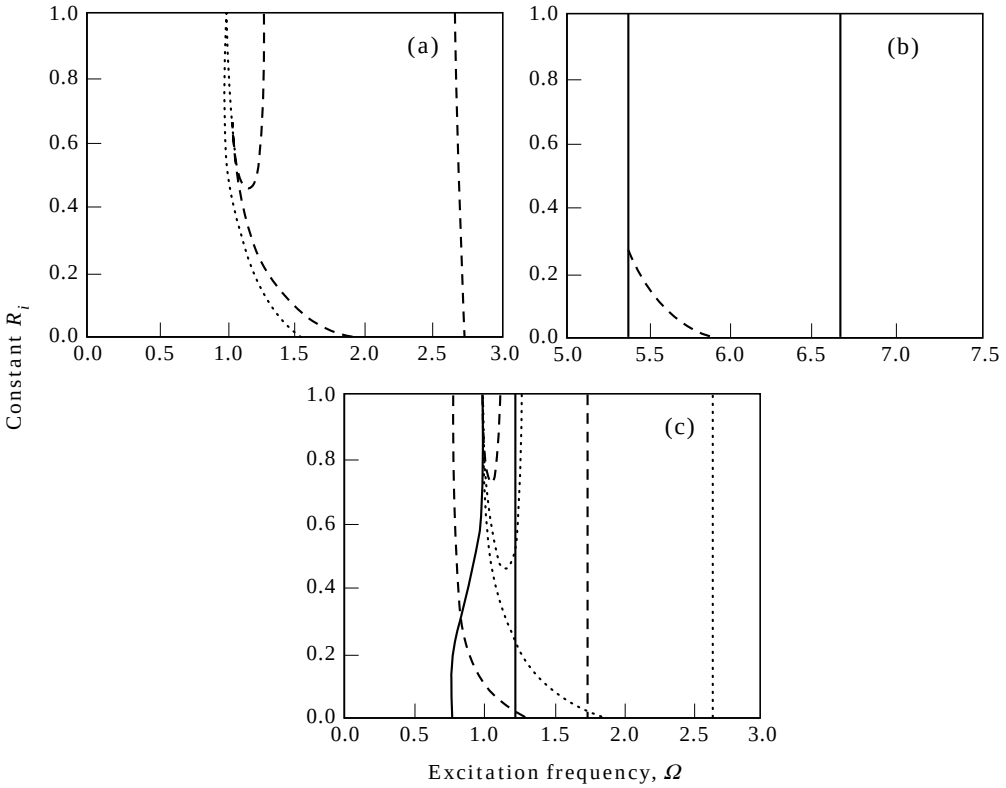

Figure 4. Effect of amplitude of sinusoidal force on the stability regions of: (a) (1, 1) for $F = 0{\cdot}01$, ·····; and 100·0, ----; (b) (1, 3) for $F = 0{\cdot}01$, ——; and 100·0, -----, for $S_1 = 0{\cdot}0$; and (c) (1, 1) motion for $F = 0{\cdot}5$, ——; 2·0, -----; and 100, ·····, for $S_1 = 1$.

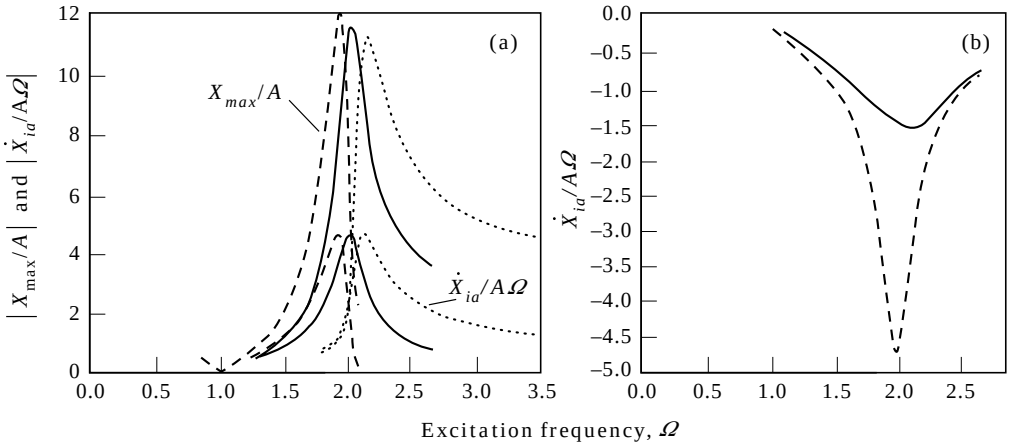

Figure 5. Effect of Ω and bias force F_0 on X_{max}/A and $\dot{X}_{ia}/A\Omega$ for: (a) constant $R_i = R_0 = 0{\cdot}8$ and $F_0 = 0{\cdot}0$, ——; $0{\cdot}3$, ·····; $-0{\cdot}3$, -----; and (b) on $\dot{X}_{ia}/A\Omega$ for velocity dependent coefficient of restitution based on equation (8a) for $k_1 = 0{\cdot}1$, -----; and $k_1 = 0{\cdot}0$, ——; at $S_1 = 0$ and $F = 1{\cdot}0$.

performed using double precision arithmetic. Theoretical predictions agreed with results obtained using a simulation approach and with previous results, and are presented next.

3. RESULTS AND DISCUSSION

Results were obtained using values of K, M, F, F_0 and ξ as 1, 1, 1, 0 and 0·05, respectively, unless stated otherwise. Theoretical predictions of complex motions based on equations (9) and (10), two unequispaced and two and one equispaced impacts per period of motion based on equations (12)–(14) were compared with results obtained using a numerical simulation approach and, wherever possible, with previous results, and they all concurred. A periodic motion repeating after N impacts in k cycles of external sinusoidal force will be identified by (N, k). Four cases are considered, namely, the oscillator contacting a single stop having unequispaced (2, 1) and second period doubling (4, 4), and the oscillator contacting two stops exhibiting alternating unequispaced (2, 1) with unequal gaps and (4, 1) motion with two consecutive impacts on each side with identical gaps. Theoretical predictions and simulation results of these four cases are presented in Table 1 and they agree. The period doubling motion presented as a second case in Table 1 also looks similar to previous results [20]. Additionally, results with the velocity dependent coefficient of restitution were also obtained for an oscillator contacting a single stop with the following parameters: $N = 6$, $\Omega = 0{\cdot}5$, $d_i = 0$, $\xi = 0$, $F = 5{\cdot}0$ and $R_i = 0{\cdot}8(1 - 0{\cdot}05\dot{X}_{ib})\dot{X}_{ib}$. Stable periodic (6, 1) motion was obtained and values of $\Omega t_i + \tau$ and $\dot{X}_{ib}$ were 0·0089, 1·0713, 1·6525, 2·0726, 2·4254, 2·7721 and 6·7769, 5·2860, 3·2296, 2·0812, 1·3609 and 0·8423, respectively. Eigenvalues of matrix P were $-0{\cdot}0039$ and $-0{\cdot}3678$ which indicated that motion was stable. Simulation results with $x_0 = -3$ and $\dot{x}_0 = -1$ were exactly identical to those reported above. To exemplify the wide variety of motions which can be theoretically studied, cases presented in Table 1 and the just mentioned velocity dependent coefficient of restitution case are shown in Figures 2(a)–(e), respectively. Additionally for an undamped oscillator hitting a stop situated at zero gap, and using values of system parameters identical to those used by Shaw and Holmes, the bifurcation values of Ω_1, Ω_2 and Ω_3 obtained using equation (10) were 2·65334, 2·71598

and 2·72911, respectively, and they agreed with previous results [20]. The same Ω_1 and Ω_2 were obtained using the closed form expressions (12) and (13), respectively.

Examination of equations (10)–(13) indicates that gap related terms appear only as $d_i - F_0/K$ and equal effective gaps $S_1 - F_0/K$ or $S_2 + F_0/K$ and this indicates that effective gaps control the dynamics. Hence the third case presented in Table 1 was also studied using gaps of $S_1 = 1{\cdot}05$, $S_2 = 1{\cdot}0$ and $F_0 = 0{\cdot}05$. Results obtained using equations (10)–(12) and simulation were identical to those given in Table 1 and this confirms the above observation. Many times precompression is used to avoid impacts and can be considered as a special case of zero gap with bias force. As an example, pre-compression X_p on side one is dynamically equivalent to $S_1 = 0$, $F_0 = KX_p$ or $S_1 = -X_p$ and $F_0 = 0$. A case with $R_1 = 0{\cdot}5$, $\Omega = 1{\cdot}0$ and $X_p = 0{\cdot}1$ was studied using theory and simulation using two sets of values: $S_1 = 0$, $F_0 = 0{\cdot}1$ and $S_1 = -0{\cdot}1$ and $F_0 = 0$. Both methods indicated that stable (2, 1) motion occurred with $\Omega(t_{i+1} - t_i)/2\pi$ and $\dot{X}_{ia}$ as 0·2156, 0·7844 and $-0{\cdot}8560$, $-0{\cdot}3592$, respectively. In summary, theoretical predictions of complex periodic motions agreed between themselves and with simulation results and previous results. The dynamics of the impact oscillator with a single stop was considered first and is followed by a two stops case.

Effects of bias force F_0 and damping ξ on equispaced (1, 1) and (1, 3) motions of impact oscillator contacting a single stop with zero gap are shown in Figures 3(a)–(d), respectively. Figure 3(a) indicates that stability regions of $F_0 \neq 0$ when compared to the case of $F_0 = 0$ move towards the right and left respectively for $F_0 > 0$ and $F_0 < 0$. The effect of F_0 on (1, 3) (see Figure 3(b)) can be significant as even the small $F_0 = 0{\cdot}025$ has a similar effect as that of $F_0 = 0{\cdot}2$ on (1, 1). This indicates that the bias force may play a major role in the high frequency response of an oscillator. The effect of damping ξ (see Figure 3(c)) indicates that the right boundary of the stability region of (1, 1) moves to the right and the valley region near the left boundary moves upwards with an increase in ξ as compared to the region of $\xi = 0$. The effect of increasing damping on (1, 3) stability regions is compared to that of $\xi = 0$ in Figure 3(d) and it indicates a slight enlargement of the stability region with increasing damping and thus the effect of small change in damping on stability regions is not significant. The effect of large change in amplitude of the sinusoidal force F on stability regions of (1, 1) and (1, 3) for $F = 0{\cdot}01$ and 100 at $S_1 = 0$ and on (1, 1) for $F = 0{\cdot}5$,

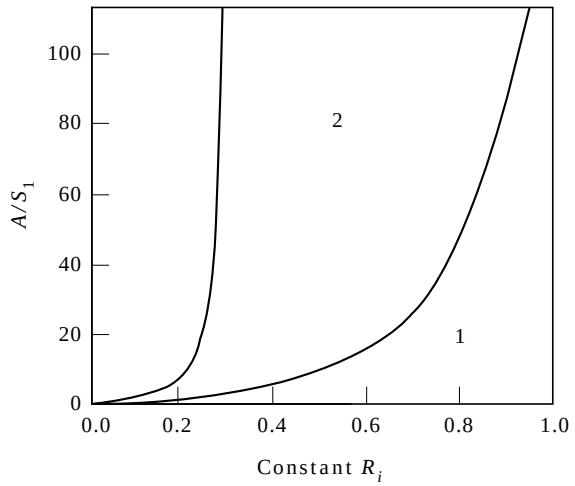

Figure 6. Stability regions of (1, 1) and (2, 1) motions with constant coefficient of restitution at $\Omega = S_1 = 1{\cdot}0$. The number of impacts is indicated by the corresponding number in this and other figures that follow.

2·0 and 100 at $S_1 = 1$ is shown in Figures 4(a)–(c), respectively. Careful comparison of Figure 4(a) with 3(a) indicates that only the left stability boundary is somewhat affected and moves towards the right with an increase in the force level. The corresponding left boundary for the (3, 1) motion shown in Figure 4(b) is nearly vertical for $F = 0{\cdot}01$ and thus the stability region of this motion expands below $R \approx 0{\cdot}25$ with decreasing force.

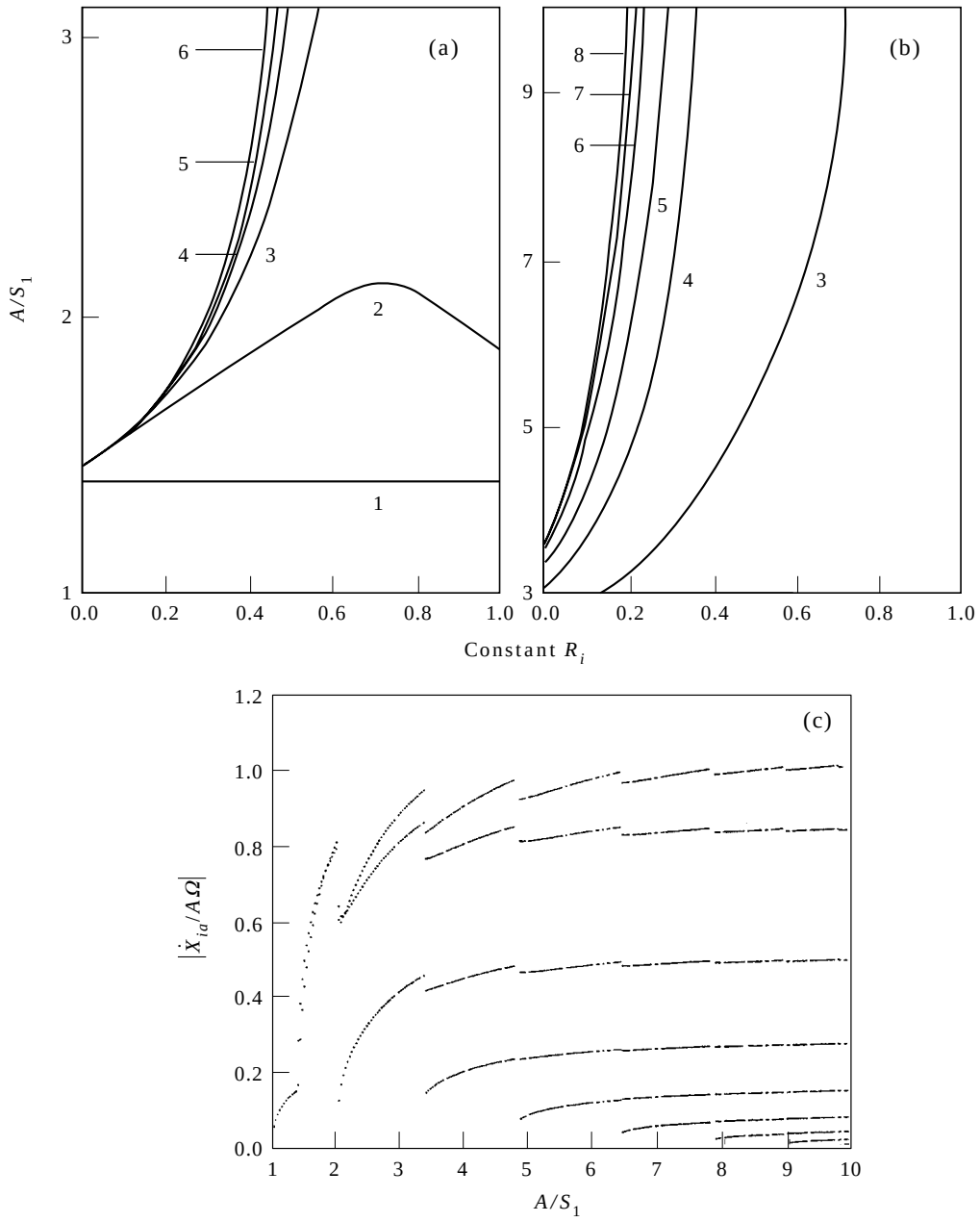

Figure 7. Stability regions of $(N, 1)$ motions for $\Omega = 0{\cdot}5$ are shown in two figures: (a) $A/S_1 \leqslant 3$; (b) $A/S_1 \geqslant 3$; and (c) variation in $\dot{X}_{ia}/A\Omega$ at $R_i = 0{\cdot}6$. C and G in this and figures that follow indicate a complex motion and a joint motion respectively.

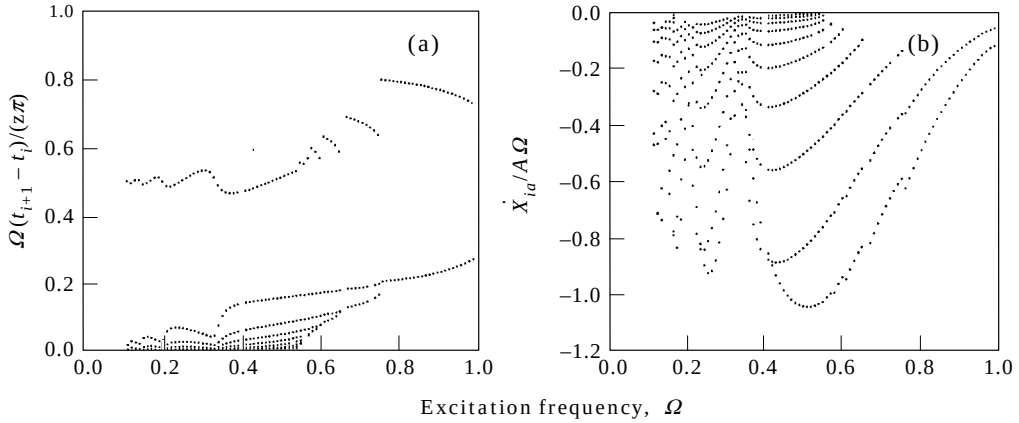

Figure 8. Variation in: (a) $\Omega(t_{i+1} - t_i)/(2\pi)$; and (b) $\dot{X}_{id}/A\Omega$ with Ω during complex periodic motions occurring for $\Omega \leqslant 1{\cdot}0$ at constant $R_i = 0{\cdot}6$.

These figures also indicate that right boundaries coincide even though the force was increased 10,000 times from 0·01 to 100. This indicates that for a stop on one side with zero gap, the stability regions of (1, 1) motions change slightly with the force level in this case. A comparison of the results shown in Figure 4(c) to those in Figure 4(a) indicates that a non-zero gap affects the stability region at a small force level to a greater extent than at the larger force level. Comparison of Figure 3(a) to Figure 4(c) clearly indicates that the (1, 1) stability region for $F = 1$, gap $= 0$ and that for $F = 100$, gap $= 1$ are nearly identical. Hence stability regions for the zero gap case can be useful to predict approximately the stability regions of (1, 1) motions with non-zero gaps when impactless displacement A is much larger than the gap.

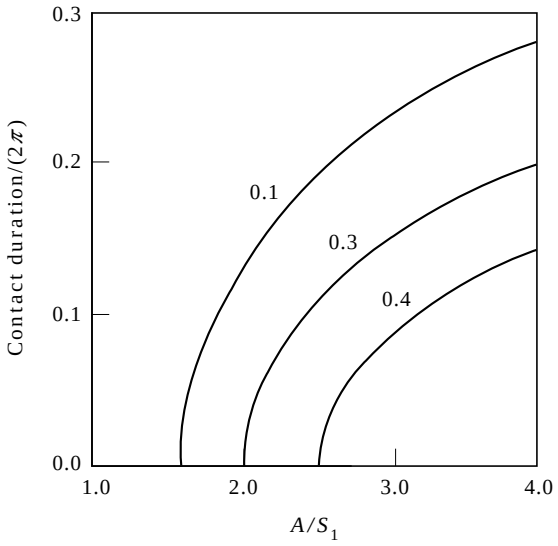

Figure 9. Variation in non-dimensional contact duration during joint motion at $\Omega = 1{\cdot}5$ with A/S_1 for $R = 0{\cdot}1$, 0·2 and 0·4.

Often snubbers and bias force are used to reduce the maximum displacement. The variation of nondimensional displacement X_{max}/A and velocity $\dot{X}_{ia}/A\Omega$ with Ω is shown in Figures 5(a) and (b) for constant and velocity dependent coefficient of restitution, respectively. A bias force acting towards the wall slightly decreases the maximum displacement and peak velocity remains nearly constant. Wear of impacting surface depends on impact velocity and hence reduction in displacement with the use of a small bias force may be slightly beneficial. However, the use of a positive bias force may increase the duration of joint motion and hence caution is required in its use. Figure 5(b) indicates that $\dot{X}_{ia}/A\Omega$ in the case of a velocity dependent coefficient of restitution is smaller than that when the coefficient is constant.

Stability regions of the (1, 1) and (2, 1) motions at resonance are shown in Figure 6 which indicates that (2, 1) starts at the end of (1, 1) and (2, 1) occurs also for a large force level when the coefficient of restitution is greater than 0·25. However, it differs below resonance and these stability regions of $(N, 1)$ for $N \leqslant 8$ at $\Omega = 0{\cdot}5$ are shown in separate Figures 7(a) and (b). Both figures indicate that the number of impacts increases with increase in A/S_1. Additionally, Figure 7(a) indicates that when A/S_1 is small and the coefficient of restitution is low, the mass remains in contact with the wall for some time during the cycle when $\Omega < \omega_n$. Variation of $\dot{X}_{ia}/A\Omega$ with A/S_1 at $e = 0{\cdot}6$ is shown in Figure 7(c) which indicates that when A/S_1 is large, the $\dot{X}_{ia}/A\Omega$ reaches 1·0 and is followed by a sequence of rapidly occurring impacts with decreasing impact velocity. Motions when A/S_1 is large looked very similar to that shown in Figure 2(e). It was also observed that below resonance, complex multi-impact periodic motions occur with two or more impacts per cycle and corresponding variation of $\dot{X}_{ia}/A\Omega$ and $\Omega(t_{i+1} - t_i)/(2\pi)$ with Ω is shown in Figure 8(a) and (b), respectively. The 2, 3, 4 and 5 impacts/cycle motions take place in the excitation frequency ranges of 1·0–0·76, 0·75–0·67, 0·66–0·61 and 0·60–0·57, respectively. When the excitation frequency decreases below $\Omega = 0{\cdot}57$, the number of impacts increases significantly and time durations between the clustered low velocity impacts also decrease. These motions looked similar to that shown in Figure 2(e). Joint motion can also occur for $\Omega > \omega_n$ when the coefficient of restitution is small, and the corresponding variation of contact duration with A/S_1 is shown in Figure 9 for $R = 0{\cdot}1$, 0·2 and 0·4 and $\Omega = 1{\cdot}5$. However, when the system operates above resonance, joint motion rarely occurs even at moderately large force levels when the coefficient of restitution is greater than 0·5 and joint motion is generally not a significant problem in this region. Results for stops on both sides situated at equal ($S_1 = S_2$) and unequal ($S_1 \neq S_2$) clearances are presented next.

Stability regions of $(N, 1)$ motions for $S_1 = S_2$ and $N \leqslant 8$ are presented in Figures 10(a)–(c) at $\Omega = 0{\cdot}5$, 1·0 and 1·5, respectively. These figures indicate that N takes even values $2, 4, \ldots$ and increases with A/S_1. Results for slightly different clearances ($S_1 = 1{\cdot}0$ and $S_2 = 1{\cdot}1$) are presented in Figure 10(d). Complex periodic or aperiodic motions occur in between these stable regions and are indicated by C in Figure 10. Variations in $\dot{X}_{ia}/A\Omega$ and $\Omega(t_{i+1} - t_i)/2\pi$ with A/S_1 at $R = 0{\cdot}6$ are shown in Figures 11(a)–(h) for cases considered in Figures 10(a)–(d). Curves of $\dot{X}_{ia}/A\Omega$ shown in Figures 11(a)–(d) are symmetrical about the x-axis and this indicates that these motions are symmetrical and hence there are only $N/2$ curves in corresponding $\Omega(t_{i+1} - t_i)/(2\pi)$ plots. When gaps are slightly different, somewhat similar behavior is observed as seen in Figure 10(d) except for occurrence of one equispaced impact/cycle motion at small A/S_1.

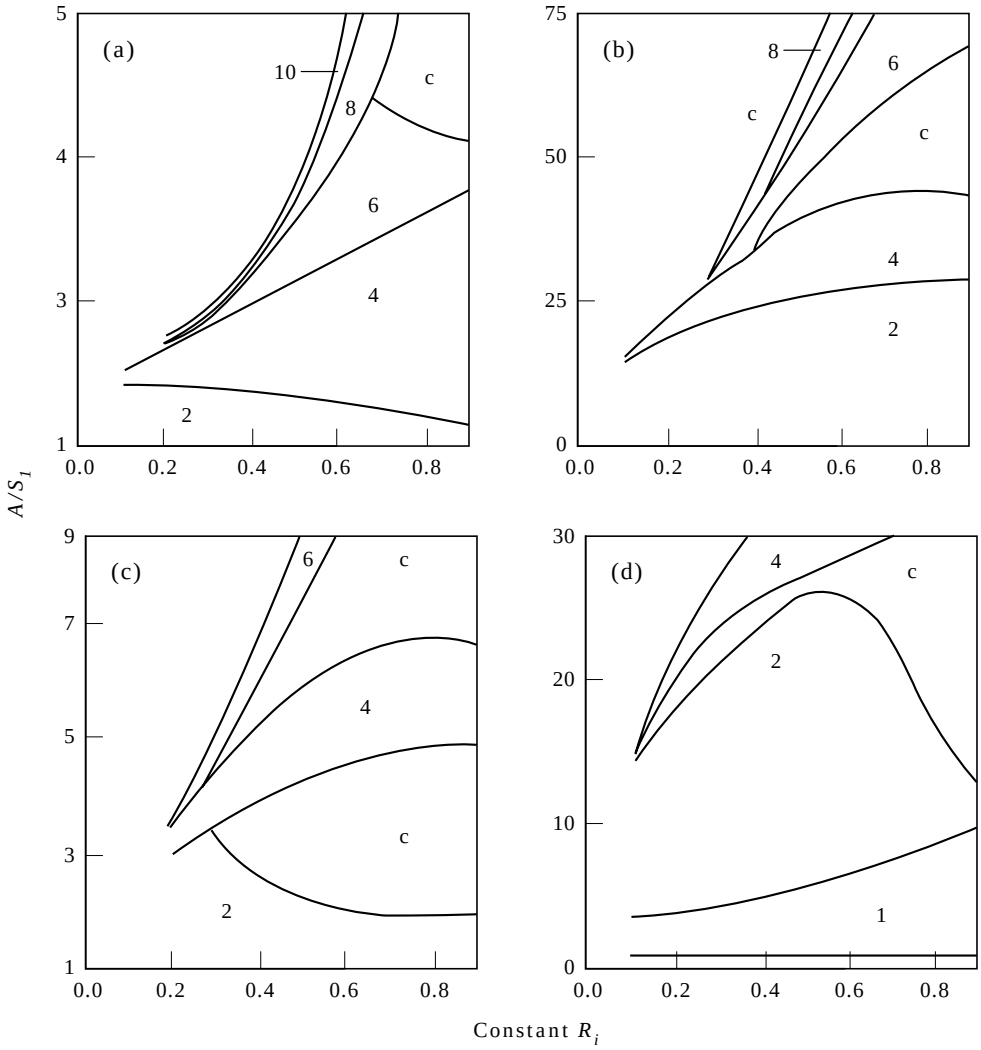

Figure 10. Stability regions of $(N, 1)$ motions for $N \leqslant 8$, $R = 0{\cdot}6$ at: (a) $\Omega = 0{\cdot}5$; (b) $\Omega = 1{\cdot}0$; (c) $\Omega = 1{\cdot}5$ with $S_1 = S_2 = 1$; (d) $\Omega = 1{\cdot}0$ with $S_1 = 1{\cdot}0$ and $S_2 = 1{\cdot}1$.

4. CONCLUSIONS

A theoretical approach to study periodic motions repeating after N impacts of a single-degree-of-freedom impact oscillator contacting rigid amplitude constraints under external sinusoidal and bias force has been developed. N non-linear equations were developed using a velocity dependent or constant coefficients of restitution representation of the impact process. These equations also govern period doubling motions. Simplified expressions for $N = 1$ and 2 are presented. Theoretical predictions concur with both previous results and those results obtained using a numerical simulation approach. The effects of amplitude and frequency of sinusoidal force, bias force, damping and variable and constant coefficients of restitution on periodic motions were investigated.

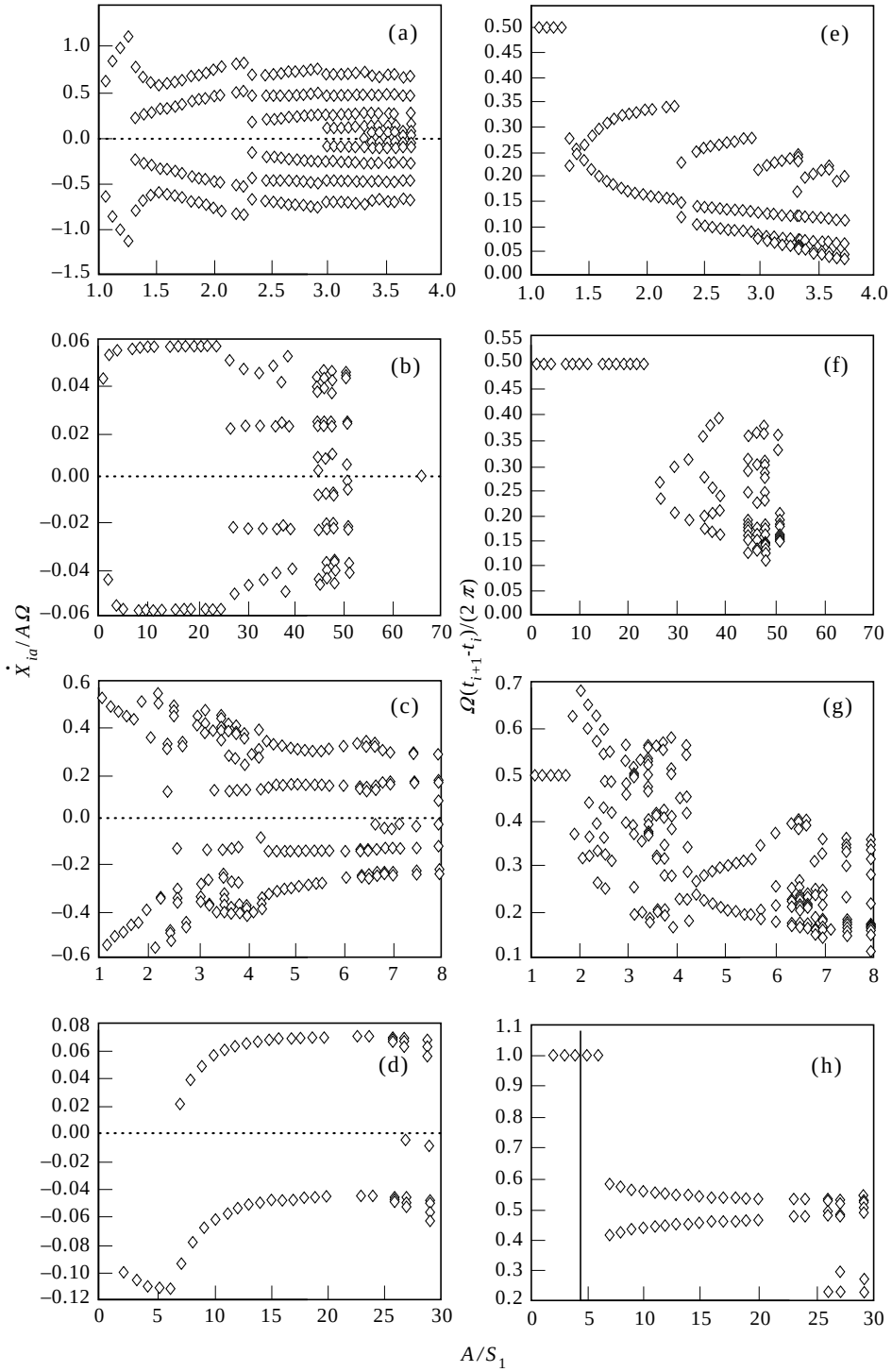

Figure 11. Variations in $\dot{X}_{ia}/A\Omega$ and $\Omega(t_{i+1} - t_i)/(2\pi)$ with A/S_1 corresponding to Figures 10(a)–(d) at $R_i = 0{\cdot}6$ are shown in (a)–(h), respectively.

ACKNOWLEDGMENT

The author gratefully acknowledges the support of a PSC-CUNY grant.

REFERENCES

1. V. I. Babitskii 1966 *Mashinovedeni* No. 1, 22–25. Existence of high frequency oscillations of large amplitudes in linear system with limiters (in Russian).
2. A. E. Kobrinskii 1969 *Dynamics of Mechanisms with Elastic Connections*. London: ILIFFE Books Ltd.
3. A. E. Kobrinskii and A. Kobrinskii 1973 *Vibroimpact System* (in Russian). Moscow: Nauka Press.
4. V. I. Babitskii 1978 *Theory of Vibroimpact Systems* (in Russian). Moscow: Nauka Press.
5. C. C. Fu and B. Paul 1969 *Journal of Engineering for Industry*, *Transactions of The American Society of Mechanical Engineers B* **91**, 1175–1179. Dynamic stability of a vibrating hammer.
6. M. Senator 1970 *Journal of Acoustical Society of America* **47**, 1390–1397. Existence and stability of periodic motions of a harmonically forced impacting systems.
7. F. Hendriks 1983 *IBM Journal* **27**, 273–280. Bounce and chaotic motion in impact print hammers.
8. S. F. Masri 1978 *Journal of Mechanical Design*, *Transactions of The American Society of Mechanical Engineers* **100**, 480–486. Analytical and experimental studies of a dynamic system with a gap.
9. G. S. Whiston 1979 *Journal of Sound and Vibration* **67**, 179–186. Impacting under harmonic excitation.
10. G. S. Whiston 1983 *Journal of Sound and Vibration* **86**, 557–562. An analytical model of two-dimensional impact/sliding response to harmonic excitation.
11. G. S. Whiston 1987 *Journal of Sound and Vibration* **118**, 395–425. Global dynamics of a vibro-impacting linear oscillator.
12. J. M. T. Thompson and R. Ghaffari 1982 *Physics Letters* **91A**, 5–8. Chaos after period-doubling bifurcations in the resonance of an impact oscillator.
13. J. M. T. Thompson and R. Ghaffari 1983 *Physical Review A* **27**, 1741–1743. Chaotic dynamics of an impact oscillator.
14. J. M. T. Thompson and J. S. N. Elvey 1983 *International Journal of Mechanical Science* **26**, 419–425. Elimination of sub-harmonic resonance of compliant marine structures.
15. J. M. T. Thompson, A. R. Bokaian and R. Ghaffari 1983 *IMA Journal of Applied Mathematics* **31**, 207–234. Subharmonic resonance and chaotic motions of a bilinear oscillator.
16. F. C. Moon 1980 *Journal of Applied Mechanics*, *Transactions of The American Society of Mechanical Engineers* **47**, 638–644. Experiment on chaotic motions of a forced nonlinear oscillator: strange attractors.
17. S. W. Shaw and P. J. Holmes 1983 *Journal of Applied Mechanics*, *Transactions of the American Society of Mechanical Engineers* **50**, 849–857. A periodically forced impact oscillator with large dissipation.
18. S. W. Shaw and P. J. Holmes 1983 *Physical Review Letters* **51**, 623–626. Periodically forced linear oscillator with impacts: chaos and long period motion.
19. S. W. Shaw 1985 *Journal of Applied Mechanics*, *Transactions of The American Society of Mechanical Engineers* **52**, 453–464. The dynamics of a harmonically excited system having rigid amplitude constraints.
20. S. W. Shaw and P. J. Holmes 1983 *Journal of Sound and Vibration* **90**(1), 129–155. A periodically forced piecewise linear oscillator.
21. C. N. Bapat and S. Sankar 1985 *Journal of Vibration*, *Acoustics*, *Stress and Reliability in Design*, *Transactions of the American Society of Mechanical Engineers* **107**, 347–350. Exact analysis of an oscillator hitting a stop.
22. D. T. Nguyen, S. T. Noah and C. F. Kettleborough 1986 *Journal of Sound and Vibration* **109**, 293–325. Impact behaviour of an oscillator with limiting stop—Part I: A parametric study. Part II: Dimensionless design parameters.
23. Y. S. Choi and S. T. Noah 1988 *Journal of Sound and Vibration* **121**, 117–126. Forced periodic vibration of unsymmetric piecewise-linear systems.

24. G. R. Tomlinson and J. Lam 1984 *Journal of Sound and Vibration* **96**, 111–125. Frequency response characteristics of structures with single and multiple clearance-type non-linearity.
25. I. Abu Mahfouz and F. Badrakhan 1989 *Journal of Sound and Vibration* **143**, 255–328. Chaotic behaviour of some piecewise-linar systems. Part I: Systems with set-up spring or with unsymmetric elasticity. Part-II: Systems with clearance.
26. A. B. Nordmark 1991 *Journal of Sound and Vibration* **145**, 279–297. Non-periodic motion caused by grazing incidence in an impact oscillator.
27. Ch. Glocker and F. Pfeiffer 1992 *Nonlinear Dynamics* **3**, 245–259. Dynamical systems with unilateral contacts.
28. A. Kahraman 1992 *Nonlinear Dynamics* **3**, 183–198. On the response of a preloaded mechanical oscillator with a clearance: period doubling and chaos.
29. C. N. Bapat and S. Sankar 1985 *Journal of Sound and Vibration* **103**, 457–469. Multi-unit impact damper—re-examined.
30. Y. Tatara and N. Moriwaki 1992 *Bulletin of the Japan Society of Mechanical Engineers* **25**, 631–637. Study of impact of equivalent two bodies (coefficient of restitution of spheres of brass, lead, glass porcelain and agate and the material properties).
31. H. P. Kirchner and R. M. Gruver 1978 *Materials Science and Engineering* **33**, 101–106. The effect of localized damage on energy losses during impact.
32. Harwell Subroutine Library 1979 Computer Science and Systems Division, AERE Harwell Oxfordshire, U.K. AERE-R 9185.

APPENDIX A: DEFINITIONS, COEFFICIENTS AND MATRIX ELEMENTS

The undefined variables in the main text are explicitly defined here:

$$\xi = C/2(KM)^{1/2}, \qquad r = \Omega/\omega, \qquad \omega = (K/M)^{1/2}, \qquad \alpha_1 = 0, \qquad a_i = \Omega t_i,$$

$$\eta = (1-\xi^2)^{1/2}, \qquad A = (F/K)/[(1-r^2)^2 + (2\xi r)^2]^{1/2}, \qquad \psi = \tan^{-1}[2\xi r/(1-r^2)],$$

$$b_i = X_i - A\sin(\alpha_i - \psi) - F_i/K, \qquad a_i = (1/\eta)\{(1/\omega)\dot{X}_{ia} - Ar\cos(\alpha_i - \psi) + \xi b_i\},$$

$$E_t = \exp[-(\xi/r)(\Omega t - \alpha_i)], \qquad \tau = \Omega t_1 - \psi, \qquad \phi_t = (\eta/r)(\Omega t - \alpha_i), \qquad C_{1t} = E_t \sin\phi_t,$$

$$C_{2t} = E_t \cos\phi_t, \qquad C_{3t} = \omega(\eta C_{2t} - \xi C_{1t})$$

and

$$C_{4t} = -\omega(\xi C_{2t} + \eta C_{1t}).$$

Values of E_i and ϕ_i are obtained by substituting i for t and α_{i+1} for Ωt in the left and right hand sides of the concerned equations respectively. C_{1i}–C_{4i} can be obtained by changing t to i on both sides of these expressions. Additional coefficients q_1–q_6 which are required in equation (12) are given below.

$$q_1 = \sin\alpha_2 [R_2 C_{31}/C_{11} - \xi\omega - \eta\omega C_{22}/C_{12}] - \Omega(1+R_2)\cos\alpha_2,$$

$$q_2 = \cos\alpha_2 [R_2 C_{31}/C_{11} - \xi\omega - \eta\omega C_{22}/C_{12}] + \Omega(1+R_2)\sin\alpha_2 + \eta\omega/C_{12} + R_2(C_{41} - C_{31}C_{21}/C_{11}),$$

$$q_3 = (S_1 - F_0/K)[\eta\omega/C_{12} + R_2(C_{41} - C_{31}C_{21}/C_{11})] + (-S_2 - F_0/K) \times [R_2 C_{31}/C_{11} - \xi\omega - \eta\omega C_{22}/C_{12}],$$

$$q_4 = \sin\alpha_2 [R_1(C_{42} - C_{32}C_{22}/C_{12}) + \eta\omega/C_{11}] - \Omega(1+R_1),$$

$$q_5 = \cos\alpha_2 [R_1(C_{42} - C_{32}C_{22}/C_{12}) + \eta\omega/C_{11}] + [R_1 C_{32}/C_{12} - \xi\omega - \eta\omega C_{21}/C_{11}],$$

$$q_6 = (-S_2 - F_0/K)[\eta\omega/C_{11} + R_1(C_{42} - C_{32}C_{22}/C_{12})] + (S_1 - F_0/K) \times [R_1 C_{32}/C_{12} - \xi\omega - \eta\omega C_{21}/C_{11}].$$

Elements of a stability governing matrix P_i are given below with few new variables:

$$U_{1i} = C_{3i}\, a_i\, /\Omega + C_{4i}\, b_i\, /\Omega + A\cos(\alpha_{i+1} + \tau),$$

$$U_{2i} = a_i\,(\eta C_{4i} - \xi C_{3i})/r + b_i\,(-\eta C_{3i} - \xi C_{4i})/r - A\Omega\sin(\alpha_{i+1} + \tau),$$

$$U_{3i} = -a_i\,(\eta C_{4i} - \xi C_{3i})/r - b_i\,(-\eta C_{3i} - \xi C_{4i})/r - AC_{4i}\cos(\alpha_{i+1} + \tau) + AC_{3i}\,(r\sin(\alpha_i + \tau) - \xi\cos(\alpha_i + \tau))/\eta,$$

$$P_i(1,1) = [C_{3i}\, a_i\, /\Omega + C_{4i}\, b_i\, /\Omega - AC_{1i}\,(r\sin(\alpha_i + \tau) - \xi\cos(\alpha_i + \tau))/\eta + AC_{2i}\cos(\alpha_i + \tau)]/U_{1i},$$

$$P_i(1,2) = -C_{1i}\,/(\eta\omega U_{1i}), \qquad P_i(2,1) = -R_{i+1}\,[U_{2i}\,P_i(1,1) + U_{3i}),$$

$$P_i(2,2) = -R_{i+1}\,[U_{2i}\,P_i(1,2) + C_{3i}\,/(\eta\omega)].$$

For the velocity dependent coefficient of restitution cases where the velocity variation is given by equations (8a) and (8b), $P_i(2,1)$ and $P_i(2,2)$ can be obtained by substituting $R_0(1 - 2k_1\,\dot{X}_{(i+1)b})$ and $R_0(1 + k_2\,(k_3\,\dot{X}_{(i+1)b} - 1)\exp(-k_3\,\dot{X}_{(i+1)b})]$, respectively, for R_{i+1} in the above expressions of stability elements.

APPENDIX B: LIST OF SYMBOLS

A	displacement amplitude of M without impacts
C	viscous damping constant
S_1, S_2	gaps between M and stop 1 and 2, respectively
F	amplitude of the external sinusoidal force
K	spring stiffness
M	mass of the main system
N	number of impacts in a period T_0
P	stability governing matrix, $P_i\,P_{i+1}, \ldots, P_{i+N}$
P_i	a 2×2 matrix, relates perturbations at the $(i+1)$th impact to those at the ith impact.
R	constant coefficient of restitution
R_i	coefficient of restitution at the ith impact
R_1, R_2	constant coefficients of restitution for side 1 and 2, respectively
r	frequency ratio, Ω/ω
T_0	period of motion
t_i	time at which the ith impact occurs
$X(t)$	absolute displacement of M
X_i	displacement of M at the ith impact
X_p	pre-compression of M due to forced closure
$\dot{X}_{ia}$	velocity of M just after the ith impact
$\dot{X}_{ib}$	velocity of M just before the ith impact
X_{max}	maximum displacement of M with impacts
Ω	frequency of the external sinusoidal force
ω	natural frequency, $\sqrt{(K/M)}$
τ	phase angle between the applied force and the 1st impact
ξ	damping ratio, $C/2M\omega$
$\dot{}$	superscript, represents the time derivative.